ORIGINAL ARTICLE

Spatial patterning in PM$_{2.5}$ constituents under an inversion-focused sampling design across an urban area of complex terrain

Brett J. Tunno, Rebecca Dalton, Drew R. Michanowicz, Jessie L.C. Shmool, Ellen Kinnee, Sheila Tripathy, Leah Cambal and Jane E. Clougherty

Health effects of fine particulate matter (PM$_{2.5}$) vary by chemical composition, and composition can help to identify key PM$_{2.5}$ sources across urban areas. Further, this intra-urban spatial variation in concentrations and composition may vary with meteorological conditions (e.g., mixing height). Accordingly, we hypothesized that spatial sampling during atmospheric inversions would help to better identify localized source effects, and reveal more distinct spatial patterns in key constituents. We designed a 2-year monitoring campaign to capture fine-scale intra-urban variability in PM$_{2.5}$ composition across Pittsburgh, PA, and compared both spatial patterns and source effects during "frequent inversion" hours *vs* 24-h weeklong averages. Using spatially distributed programmable monitors, and a geographic information systems (GIS)-based design, we collected PM$_{2.5}$ samples across 37 sampling locations per year to capture variation in local pollution sources (e.g., proximity to industry, traffic density) and terrain (e.g., elevation). We used inductively coupled plasma mass spectrometry (ICP-MS) to determine elemental composition, and unconstrained factor analysis to identify source suites by sampling scheme and season. We examined spatial patterning in source factors using land use regression (LUR), wherein GIS-based source indicators served to corroborate factor interpretations. Under both summer sampling regimes, and for winter inversion-focused sampling, we identified six source factors, characterized by tracers associated with brake and tire wear, steel-making, soil and road dust, coal, diesel exhaust, and vehicular emissions. For winter 24-h samples, four factors suggested traffic/fuel oil, traffic emissions, coal/industry, and steel-making sources. In LURs, as hypothesized, GIS-based source terms better explained spatial variability in inversion-focused samples, including a greater contribution from roadway, steel, and coal-related sources. Factor analysis produced source-related constituent suites under both sampling designs, though factors were more distinct under inversion-focused sampling.

INTRODUCTION

Exposures to fine particulate air pollution (PM$_{2.5}$) have been associated with adverse health effects, including respiratory and cardiovascular disease.[1–4] PM$_{2.5}$, however, is a complex mixture of nitrates, sulfates, organic components, metals, soil/dust particles, and other compounds, each with differing toxicities. PM$_{2.5}$ composition varies substantially across urban areas,[5] and this spatial patterning—and apparent source-concentration relationships—may vary with meteorological conditions (e.g., mixing height, wind direction), particularly in areas of complex terrain.

Elucidating spatial patterns in pollutant concentrations during "peak" exposure hours (e.g., during rush hours or under inversion conditions) may lead to a better understanding of population exposure contrasts and of constituent-specific health effects.[6] For example, under temperature inversions, limited atmospheric convection and pollutant dispersion may intensify concentrations near sources, and these "peak" spatial contrasts may better characterize source-specific intra-urban exposure gradients.

Factor analytic source apportionment has been used to identify highly correlated groups of PM$_{2.5}$ constituents, usually attributable to a common source or sources. These source apportionment methods have enabled the identification of source-specific effects of PM$_{2.5}$ on respiratory and cardiovascular outcomes.[7] Normally performed to leverage temporal variance at regulatory monitors, this approach has also been used to identify spatially correlated suites of PM$_{2.5}$ constituents across urban sites.[8,9] The spatial application offers the additional advantage that factor interpretations (frequently based on a qualitative assessment of predominant source tracers loading onto each factor) can be corroborated by examining spatial patterns with respect to source distributions.

Land use regression (LUR) techniques model spatial associations between multiple source indicators (e.g., diesel traffic density, proximity to industry) and measured pollutant concentrations. LUR modeling is normally used for single pollutants, but can also be used to identify key sources associated with correlated constituent suites, or with factor scores derived from factor analysis.[9,10] In this way, LUR models can corroborate factor interpretations, more clearly identify constituent-specific

University of Pittsburgh Graduate School of Public Health, Department of Environmental and Occupational Health, Pittsburgh, Pennsylvania, USA. Correspondence: Dr. Brett J. Tunno, University of Pittsburgh, Department of Environmental and Occupational Health, Bridgeside Point, 100 Technology Drive, Room 529, Pittsburgh, PA 15219, USA.
Tel.: +1 724 288 3778. Fax: +1 412 624 3040.
E-mail: Bjt25@pitt.edu

Table 1. Summary of literature review for constituent source indicators.

Constituents	Traffic				Local/regional	Industry		Other
	Motor vehicle	Brake/tire	Soil/road dust	Diesel	Fuel/oil	Coal/ secondary	Steel making	Wood/vegetative burning
NO$_2$	3							
BC	3, 4, 5, 24			8, 13, 19, 20, 22, 24				20
Al	24		18, 19, 20, 22, 23, 25, 26	22, 24				
As			22			1, 3, 13, 16		
Ba	4	6, 10, 13, 17	13	5				
Ca	4, 5, 8	2, 6	2, 3, 5, 20, 23, 24, 26	8, 13, 20				
Cd	11	9				1		
Cr	11	9, 13	13	22		1	21	
Cu	3, 11	2, 6, 9, 13, 17	13, 18, 22	20				
Fe	4, 5, 12	2, 6, 10, 13	2, 5, 13, 18, 20, 22, 23, 25, 26	13, 19			3, 12, 18, 19, 21	
K	5		2, 25, 26					3, 14, 19, 20, 25
La	5				12			
Mg		13	23	13				
Mn		13	13, 18, 22	19		1	3, 12, 18, 19, 21	
Mo		2, 9, 13					21	
Ni	11	9			3, 4, 12, 15, 20, 22, 26	1, 7, 12		
P	8			8				
Pb	11, 12		13, 18			1	19, 21	
S	4, 12		3	8		12, 22		
Sb		6, 9, 13, 17				1		
Se						1, 3, 12, 13, 16, 22, 25		
Sr		4, 6, 9						
V	4				3, 4, 12, 15, 20, 26	7		
Zn	5, 11, 12, 26	2, 9, 13, 17	13, 18	20			12, 19, 21	

1 (Aneja et al.[46]); 2 (Apeagyei et al.[19]) 3 (Thurston et al.[33]); 4 (Lall and Thurston[43]); 5 (Zhao et al.[34]); 6 (Sternbeck et al.[24]); 7 (De Foy et al.[47]); 8 (Spencer et al.[38]); 9 (Figi et al.[20]); 10 (Gietl et al.[23]); 11 (Gunawardana et al.[42]); 12 (Hammond et al.[35]); 13 (Schauer et al.[48]; 14 (Fine PM et al.[49]); 15 (Viana et al.[44]); 16 (Salvador et al.[50]); 17 (Iijima et al.[22]); 18 (Irvine et al.[26]); 19 (Rizzo and Scheff[32]); 20 (Qin et al.[31]); 21 (Pekney et al.[36]); 22 (Ogulei et al.[30]); 23 (Lough et al.[29]); 24 (Lough and Schauer[37]); 25 (Lee et al.[27]); 26 (Li et al.[28]).

PM$_{2.5}$ sources, and ultimately improve source-specific PM$_{2.5}$ epidemiology.[9]

The Pittsburgh, PA region is characterized by complex terrain, periods of heavy traffic, and large industrial pollution sources, along with a complex meteorology that includes frequent inversion events.[11,12] These inversion events may trap both local industrial and traffic emissions in river valleys, intensifying spatial contrasts in constituent concentrations and factor sources.[13,14] Previously, we reported greater spatial contrasts in total PM$_{2.5}$ and black carbon using inversion-focused spatial sampling; here, we compare PM$_{2.5}$ composition and source contributions under "24-h weeklong" and "inversion-focused" sampling schemes. We use factor analysis to identify spatially correlated suites of constituents, variously characterized by high loadings of constituent tracers associated with key urban sources, such as traffic, industry and long-range transport, then model factor scores using LUR. Previously, we found similar source contributions under both sampling schemes, although the GIS-based urban source terms explained a greater portion of PM$_{2.5}$ variability under the inversion-focused method.[6,11] Here, we hypothesized that the inversion-focused sampling scheme would provide higher concentrations, greater spatial variation in elemental constituents, and more spatially distinct source contributions, compared with the 24-h weeklong sampling scheme.

MATERIALS AND METHODS

Study Design

Data collection methods are detailed in Shmool et al. and Tunno et al.[6,11] Briefly, GIS-based indicators of local pollution sources (e.g., proximity to industry, traffic density) and potential source-concentration modifiers (e.g., elevation) were used to systematically allocate 37 sampling locations each year, to capture spatial and source variability across the Pittsburgh metropolitan area (~150 sq. miles). Sampling units were custom-designed to capture integrated street-level samples of PM$_{2.5}$ during selected hours of the day. Instruments were programmed for specific hours of sampling using a chrontroller (ChronTrol Corporation, San Diego, CA, USA), and a tetraCal volumetric air flow calibrator (BGI Instruments, Butler, NJ, USA) was used to calibrate the flow to 4.0 liters per minute. Data on ambient temperature and relative humidity (RH) was collected in 15-minute intervals using a HOBO data logger (Pocasset, MA). During year 1 (summer 2011, winter 2012), we performed "inversion-focused" sampling wherein the programmable instruments collected PM$_{2.5}$ across "peak" hours (6 to 11am, including the morning rush hour) Monday through Friday (25 h total) over six weeklong sampling sessions. During year 2 (summer 2012, winter 2013), we performed "24-h weeklong" sampling, wherein integrated

Table 2. GIS-based source density indicators used for LUR modeling.

Source category for LUR modeling	Covariates examined (50 m to 1000 m concentric radial buffers)	Data source
Traffic density indicators	Mean density traffic (primary roads)	Pennsylvania Department of Transportation (PADOT)
	Mean density traffic (primary and secondary roads)	
	Number of signaled intersections	
Road-specific measures	Average daily traffic on nearest primary road	PADOT
	Distance to nearest major road	
	Summed length of primary roadways	
	Summed length of primary and secondary roadways	
Truck, bus, and diesel	Mean density of bus traffic	Google Transit (11/11 - 3/12)
	Distance to nearest bus route	
	Outbound and inbound trip frequency per week summed by route	
	Mean density of heavy truck traffic on nearest primary roadway	PADOT
Population	Census population density (blockgroup)	US Census Bureau (2010)
Land use/Built environment	Total area of industrial parcels	Allegheny County Assessment Data, by parcel (2011)
	Total area of commercial parcels	
	Total area of industrial and commercial parcels	
	Percent developed imperviousness	National Land Cover Dataset (NLCD, 2006)
	Land use/land cover (LULC) urban built area from orthophotography	Southwestern Pennsylvania Commission (SPC, 2011)
Industrial emissions	Mean density of total $PM_{2.5}$ emitted per meter	National Emissions Inventory (NEI, 2011)
	Mean density of total SO_2 emitted per meter	
	Mean density of total NOx emitted per meter	
	Mean density of total VOCs emitted per meter	
Transportation facilities	Distance to nearest active railroad	SPC, 2011
	Summed line length of active railroads	
	Distance to nearest bus depot	
Potential modifying factors		
Topography	Average elevation	National Elevation Dataset (NED, 2011)
Meteorology	Temperature/relative humidity	Obtained from sampler
	Frequency of inversions	Univ. of Wyoming, Dept. of Atm. Science (2011-2012)
	Wind direction and wind speed	National Oceanic and Atmospheric Association (NOAA, 2011-2012)

Table 3. Summary of summer inversion-focused and 24-h weeklong concentrations for 37 distributed sites per year, with percent above analytic LOD ($= 3 \times$ standard deviation of the analytical blanks).

	Inversion-focused			24-h weeklong			P-value between designs
	Mean (SD)	Median	% > LOD	Mean (SD)	Median	% > LOD	
$PM_{2.5}$ (µg/m³)	14.35 (3.97)	14.68	1.00	13.94 (2.01)	13.34	1.00	0.57
BC (abs)	1.64 (0.91)	1.59	1.00	1.06 (0.36)	0.96	1.00	**0.0007**
NO_2 (p.p.b.)	12.59 (6.63)	10.59	1.00	10.37 (4.53)	10.24	1.00	0.56
Constituents measured by ICP-MS (ng/m³)							
Al	36.84 (30.03)	32.93	0.81	34.34 (24.22)	29.92	0.97	0.58
As	1.76 (0.95)	1.75	0.97	1.28 (0.78)	1.00	1.00	**0.01**
Ba	13.89 (20.82)	7.47	0.49	4.14 (2.61)	3.30	0.84	**0.002**
Ca	148.55 (270.76)	84.49	0.78	156.42 (151.56)	128.13	0.97	0.95
Cd	0.25 (0.21)	0.23	0.95	0.14 (0.08)	0.13	1.00	**0.001**
Ce	0.07 (0.05)	0.05	0.92	0.07 (0.06)	0.06	1.00	0.62
Cr	3.45 (3.54)	2.12	0.95	1.06 (0.63)	0.93	1.00	< **0.001**
Cs	0.07 (0.20)	0.02	1.00	0.03 (0.04)	0.01	1.00	0.20
Cu	11.07 (9.94)	9.43	0.95	5.71 (6.10)	3.71	0.97	**0.01**
Fe	186.00 (158.27)	128.49	0.97	110.83 (86.26)	90.66	1.00	**0.01**
K	66.87 (68.99)	57.27	0.97	93.05 (55.98)	81.69	0.97	0.10
La	0.04 (0.04)	0.03	0.92	0.04 (0.03)	0.03	1.00	0.71
Mg	23.57 (30.19)	12.45	0.76	18.42 (13.89)	15.82	1.00	0.35
Mn	7.33 (7.00)	5.42	0.97	4.90 (5.42)	3.09	1.00	0.10
Mo	2.38 (2.45)	1.53	0.97	1.44 (0.94)	1.32	1.00	**0.02**
Ni	2.11 (2.01)	1.41	0.95	1.38 (1.78)	1.07	1.00	0.06
P	5.42 (3.83)	4.48	0.84	4.45 (1.54)	4.46	1.00	0.15
Pb	6.67 (6.14)	5.78	1.00	3.87 (2.20)	3.43	1.00	**0.01**
S	1013.00 (703.55)	880.82	0.97	1032.00 (353.85)	1016.22	1.00	0.95
Sb	1.37 (1.04)	1.13	0.97	1.05 (0.43)	0.96	1.00	0.09
Se	4.22 (4.95)	2.87	0.68	1.86 (1.89)	1.49	1.00	**0.003**
Sr	0.99 (1.09)	0.70	0.81	1.05 (0.67)	0.84	0.97	0.86
Tl	0.10 (0.17)	0.04	1.00	0.07 (0.14)	0.03	1.00	0.42
V	0.52 (0.25)	0.52	0.97	0.49 (0.15)	0.45	1.00	0.37
Zn	64.16 (103.26)	36.37	0.95	23.79 (14.97)	21.44	1.00	**0.02**

The *P*-value is from a paired *t*-test comparing inversion-focused and 24-h weeklong concentrations. Bolded *P*-values indicate a significant difference ($P < 0.05$) between inversion-focused and 24-h weeklong sample designs.

samplers ran for 15 min per hour for 7 days (42 h total), over six sampling sessions. A limitation is that, owing to limited equipment availability, inversion-focused and 24-h weeklong measurements were conducted in successive years, creating non-contemporaneous measurements for comparison. To establish comparability across years, we repeated a random subset of 13 sites both years for both campaigns. A reference site located at Settlers Cabin Park in Carnegie, PA, approximately 9 miles upwind of the study area, was used throughout sampling to assess comparability across designs, and to adjust distributed samples for intra-season temporal variance.

Sample Analyses

Teflon filters (37mm; Pall Life Sciences) were pre- and post-weighed using an ultramicrobalance (Mettler Toledo Model XP2U) inside a temperature- and relative humidity-controlled glove box (PlasLabs Model 890 THC). Black carbon (BC) was measured from each filter using an EEL43M Smokestain Reflectometer (Diffusion Systems Limited, London, England),[15] and reported in absorbance units (abs). To determine elemental composition, inductively coupled plasma mass spectrometry (ICP-MS) analyses were conducted by the Wisconsin State Laboratory of Hygiene following documented protocols (ESS INO Method 400.4; EPA Method 1638).[16] Ogawa passive badges were analyzed using water-based extraction and spectrophotometry (Thermo Scientific Evolution 60S UV-Visible Spectrophotometer, Waltham, MA, USA) for nitrogen dioxide (NO$_2$) concentrations (p.p.b.).

Source Apportionment

To interpret source factors we updated a previously published literature review of observed elemental tracers of key urban PM$_{2.5}$ sources[9,17] (Table 1). The literature search was updated using PubMed and Web of Science, and search criteria included any of: "constituents," "source apportionment," or "trace metals." We retained identified source apportionment studies performed within northeastern US cities, or source-specific controlled studies (i.e., source characterizations), performed within the last three decades. Because cerium, cesium, and thallium were above LOD across nearly all sampled sites for all four seasons, we opted to retain these elements in factor analysis, although we did not originally identify clear sources in the literature review.

Following the methods outlined by Clougherty et al.[9] and Levy et al.,[17] we performed a two-stage analysis to identify groupings of correlated constituents, and to evaluate spatial relationships between factor scores and urban sources using LUR. First, we performed season-specific unconstrained factor analysis on temporally-adjusted elemental concentrations to derive factors representing latent emissions source groupings. Examining concentration variance across space, rather than time, we recognize that some constituents may have opposite spatial patterns to unrelated sources in other locations. Thus, negative loadings are plausible, and, accordingly, we opted to use unconstrained factor analysis with varimax rotation.

To determine the number of factors, we considered eigenvalue-one criterion and scree plots, and retained only those factors explaining at least 5% of total variance. Constituents loading greater than or equal to 0.60 were considered in factor interpretations. The factor solution was sensitivity-tested using constituent loading cutoffs of 0.50 and 0.70 to identify changes in factor interpretations and groupings. Statistical analyses were performed using PROC FACTOR in SAS v. 9.3 (Cary, NC, USA) and R statistical software v. 2.12.1. We used EPA's Positive Matrix Factorization model version 5.0 as a sensitivity test to corroborate our factor solution.[18]

Factor scores were calculated for each factor, across all distributed monitoring locations, for each season. We modeled factor scores as a function of GIS-based local source indicators including traffic, land use, and industry terms (Table 2). Significant GIS-based source covariates were examined to corroborate factor interpretations based on the literature

Table 4. Summary of winter inversion-focused and 24-h weeklong concentrations for 37 distributed sites per year, with percent above analytic LOD.

	Inversion-focused			24-h weeklong			P-value between designs
	Mean (SD)	Median	%>LOD	Mean (SD)	Median	%>LOD	
PM$_{2.5}$ (μg/m^3)	12.76 (2.57)	12.37	1.00	11.26 (2.01)	11.12	1.00	**0.01**
BC (abs)	1.34 (0.53)	1.24	1.00	0.93 (0.35)	0.82	1.00	**0.0002**
NO$_2$ (p.p.b.)	18.84 (6.19)	16.77	1.00	15.61 (5.44)	14.73	1.00	**0.001**
Constituents measured by ICP-MS (ng/m^3)							
Al	35.20 (44.16)	24.18	0.89	15.62 (21.53)	10.32	1.00	**0.003**
As	0.76 (0.39)	0.62	1.00	0.77 (0.59)	0.58	1.00	0.94
Ba	9.04 (11.17)	3.42	0.65	11.95 (25.96)	1.44	1.00	0.53
Ca	110.00 (113.57)	64.44	0.89	278.50 (772.58)	100.9	1.00	0.29
Cd	0.21 (0.29)	0.13	1.00	0.41 (0.95)	0.17	1.00	0.22
Ce	0.11 (0.28)	0.06	1.00	0.24 (0.95)	0.03	1.00	0.45
Cr	1.69 (1.70)	1.41	0.97	1.08 (2.27)	0.43	0.97	0.25
Cs	0.06 (0.13)	0.01	1.00	0.04 (0.10)	0.01	1.00	0.49
Cu	4.24 (2.83)	3.50	1.00	3.96 (4.34)	2.77	1.00	0.74
Fe	158.71 (202.91)	87.49	1.00	259.97 (675.82)	53.38	1.00	0.39
K	99.22 (189.72)	39.12	1.00	55.79 (46.44)	40.70	1.00	0.18
La	0.06 (0.17)	0.02	0.95	0.03 (0.04)	0.02	1.00	0.14
Mg	10.48 (9.03)	8.13	0.97	16.21 (26.90)	6.40	0.97	0.06
Mn	6.94 (9.77)	3.11	1.00	9.08 (21.96)	2.14	1.00	0.59
Mo	3.58 (4.57)	2.04	1.00	1.07 (0.74)	0.87	1.00	**0.002**
Ni	1.15 (1.35)	0.65	0.97	0.54 (0.95)	0.30	1.00	**0.03**
P	5.60 (5.98)	3.76	1.00	4.06 (3.69)	2.84	1.00	0.10
Pb	4.36 (3.64)	3.15	0.97	4.21 (5.43)	2.57	1.00	0.89
S	554.95 (259.56)	487.54	1.00	485.39 (272.89)	415.27	1.00	0.27
Sb	0.87 (0.58)	0.68	1.00	0.65 (0.51)	0.53	1.00	0.09
Se	0.63 (3.98)	1.13	0.97	1.14 (1.13)	0.92	0.86	0.05
Sr	0.56 (0.60)	0.30	1.00	0.43 (0.55)	0.23	1.00	0.27
Tl	0.04 (0.05)	0.03	1.00	0.08 (0.17)	0.02	1.00	0.24
V	0.35 (0.14)	0.30	1.00	0.33 (0.41)	0.25	1.00	0.79
Zn	47.12 (64.13)	23.02	0.95	38.99 (84.12)	10.47	1.00	0.64

The P-value is from a paired t-test comparing inversion-focused and 24-h weeklong concentrations. Bolded P-values indicate a significant difference (P < 0.05) between inversion-focused and 24-h week long sample designs.

review. Separate LUR models for each factor were derived using manual forward step-wise linear regression, separately for each sampling season ($n = 4$), following LUR methods from our prior analyses.[6] Final LUR models for each seasonal, design-specific set of factor scores were determined, with all retained source covariates significant at $P < 0.05$.

RESULTS

Summary Statistics

Across the 37 monitoring locations, 27 pollutants (25 particle constituents from ICP-MS analysis, NO$_2$, and BC) were included in factor analyses for each of four sampling seasons. Concentrations
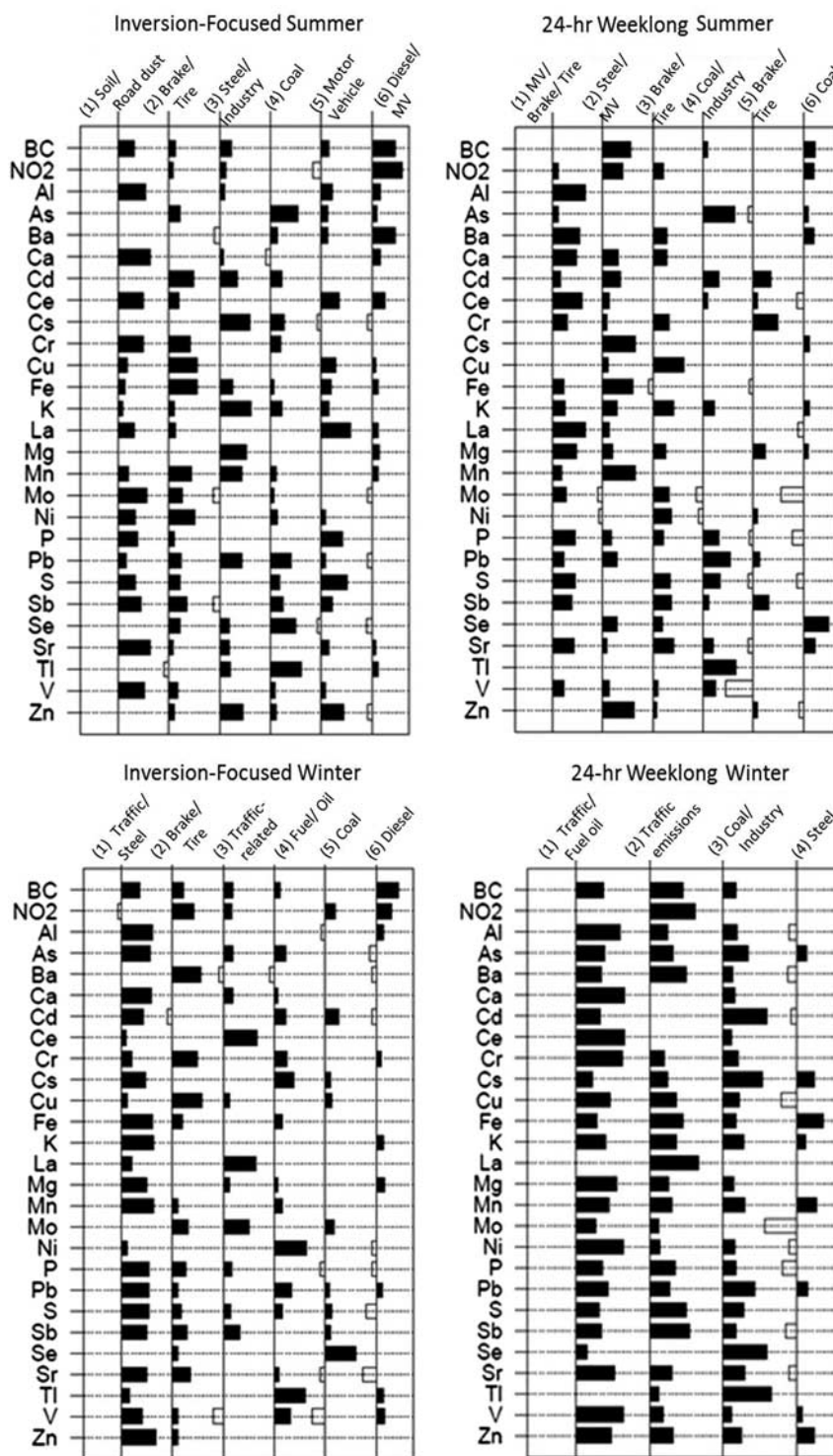
Figure 1. Factor loading plots for summer inversion-focused and 24-h weeklong constituents (top) and winter inversion-focused and 24-h weeklong constituents (bottom).

from summer inversion-focused and 24-h weeklong sampling are summarized in Table 3; concentrations from winter inversion-focused and 24-h weeklong sampling are summarized in Table 4. The highest constituent concentrations were found for aluminum (Al), calcium (Ca), iron (Fe), potassium (K), sulfur (S), and zinc (Zn), under either sampling design. Correlation matrices of elemental constituents, by season, can be found in Supplementary Material (Supplementary Tables S1 to S4). For the 13 sites repeated in both years (i.e., using both sampling designs), PM₂.₅ and BC concentrations did not significantly differ, and likewise mean concentrations at the reference monitors were comparable across years.

Literature Review

Reviewed studies[19–44] identified PM₂.₅ constituents commonly associated with a range of urban sources, including vehicular traffic: BC, Ca, Fe, Zn for motor vehicles; barium (Ba), copper (Cu), Fe, molybdenum (Mo), antimony (Sb), strontium (Sr), Zn for brake/tire wear; Al, Ca, Fe for soil/road dust resuspension; and BC, Al, Ca, Fe for diesel. Constituents commonly associated with long-range transport [e.g., arsenic (As), nickel (Ni), selenium (Se), sulfur (S)] are often associated with local coal combustion and coal-burning power plant emissions in our region. Fe, manganese (Mn), lead (Pb), and Zn are often associated with steel manufacturing; and Ni and vanadium (V) for residual fuel oil combustion (Table 1).

Factor Analysis/Source Apportionment

We identified 6-factor solutions for both summers and the inversion-focused winter constituent measures, and a 4-factor solution for the 24-h weeklong winter season (Figure 1). Similar overall variance (%) was explained by inversion-focused factor solutions compared with 24-h weeklong, especially between the summers. More traffic-related sources were identified using the inversion-focused design in both seasons, and a higher proportion of explained variance was clustered in factor one of the 24-h weeklong winter sampling.

For inversion-focused summer samples, a 6-factor solution explained 78% of overall variability across constituent concentrations (Figure 2). Factor one was characterized by indicators of *soil/ road dust* (e.g., Al, Ca). Factor two was characterized by indicators of *brake/tire wear* (e.g., Cu, Fe). Factor three included indicators of *steel-making/industry* (Cs, Mn, Pb, Zn). Factor four included *coal* (As, Se). Factor five suggested *motor vehicles* (P, Zn), and factor six indicated *diesel/motor vehicles*, given high loadings of BC and NO₂.

For 24-h weeklong summer samples, a 6-factor solution explained 78% of variability across constituents (Figure 3). Factor one included *motor vehicle* (Al, Ca, P) and *brake/tire wear* indicators (Ba, Ca, Ce, La, Mg). Factor two indicated *steel-making and motor vehicle sources* (BC, Cs, Fe, Mn, Zn). Factor three included *brake and tire wear* (Cu, Sr). As, Pb, and Tl, indicators of *coal* and *industrial emissions*, loaded strongly onto factor four. Factor five was characterized by indicators of *brake/tire wear* (Ca, Cr), and factor six included an indicator of *coal* (Se).
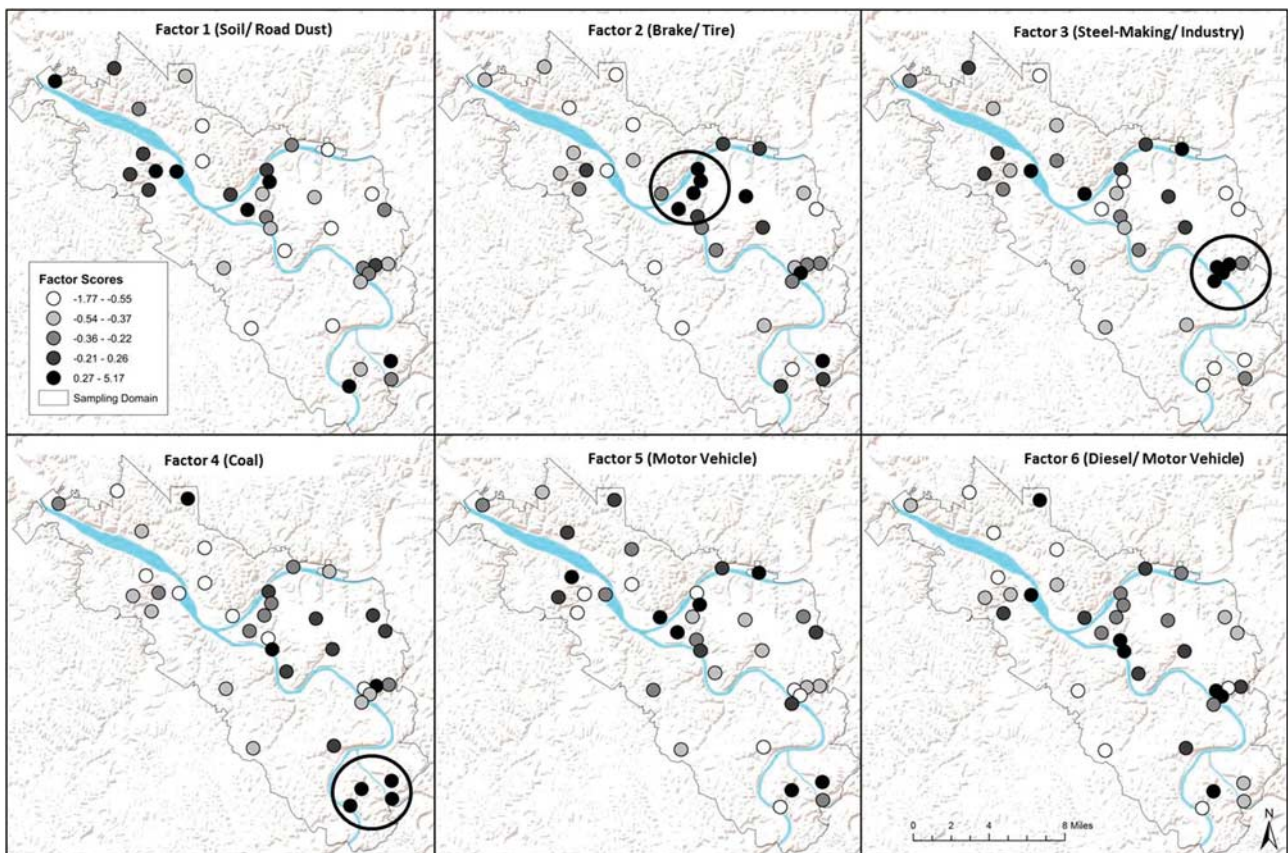

Figure 2. Spatial distribution of factor scores across monitoring locations for *inversion-focused summer sampling*, based on proposed 6-factor solution. For factor 2 (brake/tire), the circled highest concentration sites indicate areas located near downtown Pittsburgh. For, factor 3 (steel-making/industry), the circled highest concentrations indicate areas located near an active steel mill. For factor 4 (coal), the circled highest concentration sites indicate areas located near an active coke works.
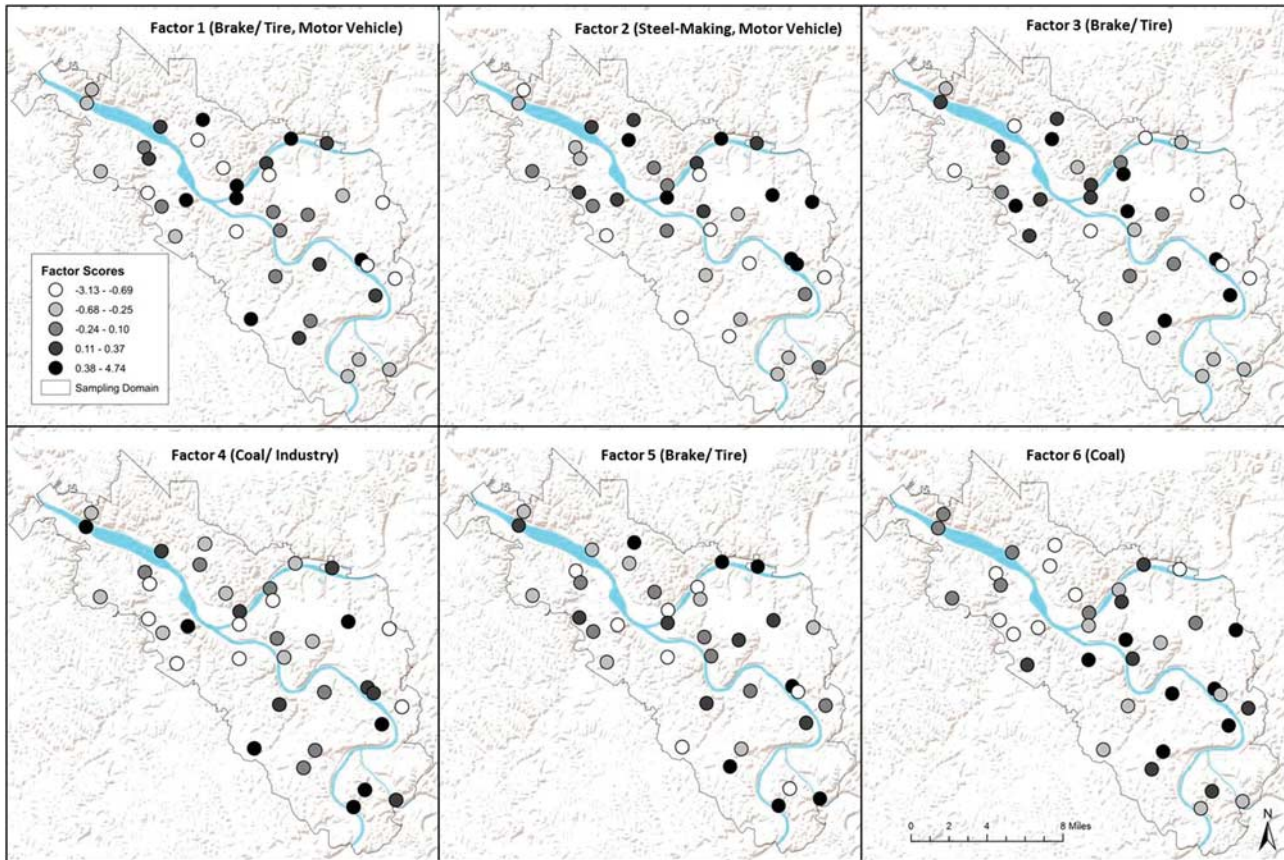
Figure 3. Spatial distribution of factor scores across monitoring locations for *24-h weeklong summer sampling,* based on proposed 6-factor solution.

For inversion-focused winter samples, a 6-factor solution explained 77% of variability found in constituents, and multiple *traffic-related* sources and *steel-making* were represented in the first factor (Figure 4). Factor two suggested *brake/tire wear*, as Ba and Cu loaded strongly. Factor three consisted of Ce, La, and Mo, suggesting that this factor may be *traffic-related*. La is associated with fuel oil combustion and motor vehicle exhaust, whereas Mo indicates brake/tire wear. Factor four indicated *fuel oil combustion* (Ni). Factor five indicated *coal* (Se). Factor six indicated *diesel* (BC).

For 24-h weeklong winter samples, a 4-factor solution explained 88% of variability across constituents (Figure 5). Factor one explained 67% of the variance and suggested a combination of many *traffic* sources (motor vehicle, brake/tire, soil/road dust, diesel) and *fuel oil* (Ni, V). Factor two indicated *traffic-emissions* (i.e., NO$_2$). Factor three indicated *coal/industry* (Pb, Se, Tl). Factor four indicated *steel-making* (Fe, Mn, Zn).

Sampling Design Comparison

The inversion-focused sampling design, on average, produced higher constituent concentrations, during both the summer and winter seasons, compared with the 24-h weeklong sampling. For the *summer*, BC (diesel/motor vehicle), As and Se (coal/secondary), Ba, Cd, Cr, Cu, and Mo (brake/tire wear), and Fe, Pb, and Zn (steel-making) concentrations were significantly higher in inversion-focused samples compared with 24-h weeklong samples. For the *winter*, PM$_{2.5}$, BC, and NO$_2$ (motor vehicle), Al (soil/road dust), Mo (brake/tire wear), and Ni (fuel/oil) concentrations were significantly higher in inversion-focused samples compared with 24-h week-long samples.

Seasonal Comparison

Within each sampling design, higher concentrations of As, S, and Tl (coal), Cu, Mg, Sb, and Sr (brake/tire wear), Ni and V (fuel oil combustion), and Pb (steel-making or soil/road dust resuspension) were found in inversion-focused samples during summer compared with the winter. Higher concentrations of Al and K (soil/road dust resuspension), As, S, and Se (coal), Ni and V (fuel oil combustion), and Sb and Sr (brake/tire wear) were found for 24-h weeklong samples during summer compared to winter (Supplementary Tables S5 and S6). Although K is often used as an indicator of wood burning, we did not find higher concentrations during winter.

LUR of Factor Scores

For inversion-focused summer samples, length of primary and secondary roadways explained variability in the *brake/tire wear* factor, and higher factor scores were observed at sites near downtown compared with those further away (Figure 2). Industrial land use within 750 m was significant for the *steel-making/industry* factor (Table 5), and higher scores were observed at sites in Braddock, PA, near an active steel mill (Figure 2). Sulfur dioxide (SO$_2$) emissions was a significant predictor for the *coal* factor (Table 5), and higher scores were observed in the Clairton/Liberty area, near an active coke works (Figure 2). Mean density of primary roadways within 1000 m was a significant predictor for the *motor vehicle* factor (Factor 5).

For 24-h weeklong summer samples, mean density of buses within 750 m was significant in the LUR model for the *motor vehicle/brake and tire wear* factor (Table 5). Commercial and industrial land use within 1000 m was significant for the *steel-making/motor vehicle* factor (Table 5). Signaled intersections within 500 m was a significant predictor for the *brake/tire wear*
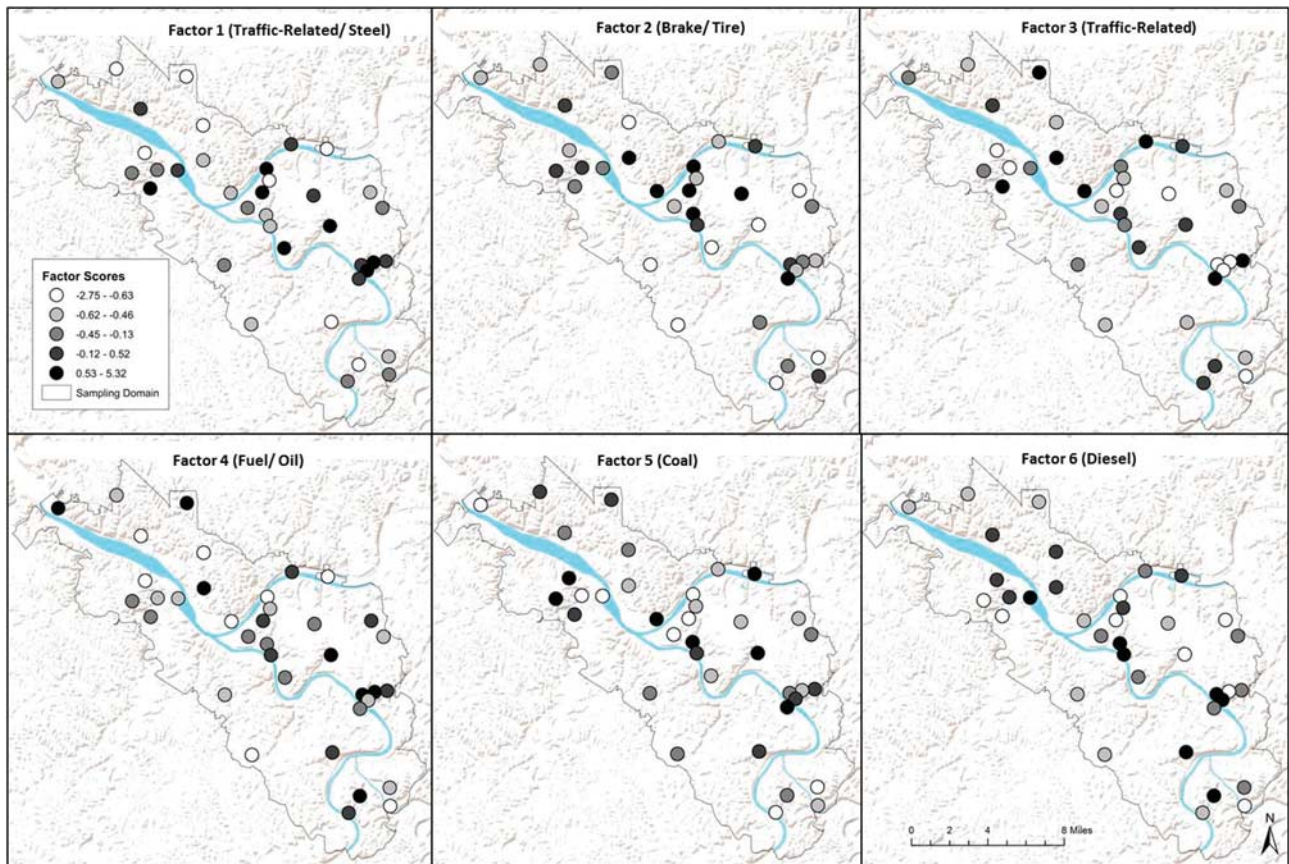
Figure 4. Spatial distribution of factor scores across monitoring locations for *inversion-focused winter sampling,* based on proposed 6-factor solution.

factor. SO$_2$ emissions was significant for the *coal industry* factor (Figure 3). No significant predictors were identified for the final *brake/tire wear and coal* factors.

For winter inversion-focused sampling, commercial and industrial land use within 500 m was significant for the *traffic and steel-making* factor (Table 6). Signaled intersections within 750 m was significant for the *brake/tire wear* factor. LUR results suggested that mean density of heavy truck traffic within 500 m and inverse distance to primary roadways were significant predictors for the *traffic-related* factor (Table 6). Elevation was the lone significant predictor for the *coal* factor, possibly indicating trapping of pollutants in the industrial river valleys during inversion-focused sampling — however, there was no significant interaction between elevation and either industrial or traffic source covariates. Signaled intersections within 500 m and summed industrial parcels within 750 m were significant for the *diesel* factor.

For 24-h weeklong winter sampling, no spatial covariates were significant for the *traffic/fuel oil* factor in LUR modeling; the most strongly correlated covariates included traffic density on primary roadways and mean truck density within 500 m ($r = 0.27$). Signaled intersections within 500 m and PM$_{2.5}$ emissions were significant LUR predictors for the *traffic emissions* factor. Industrial PM$_{2.5}$ emissions was a significant predictor for the *coal/industry* factor. Summed industrial land use within 500 m was significant for the *steel-making* factor (Table 6).

Sensitivity Analysis
Using a factor loading ⩾ 0.50 or 0.70, the elimination or addition of constituents to a factor were minimal and did not alter the proposed factor source. Therefore, results reported are at a factor

loading of ⩾ 0.60. Using EPA's Positive Matrix Factorization model, proposed seasonal factors remained similar to those determined using unconstrained factor analysis above.

DISCUSSION
PM$_{2.5}$ elemental composition was examined and compared across 37 distributed sites, across two winter and two summer seasons, using both inversion-focused and 24-h weeklong sampling methods. The inversion-focused sampling method consisted of a 5-h 6–11 am sampling period; we expected the highest frequency of inversions during these hours, where we found consistently higher PM$_{2.5}$ concentrations and a greater frequency of inversion events during morning hours in a mobile monitoring campaign.[12] Given the temporal overlap between these frequent-inversion hours and the morning rush hour, we hypothesized that this period would display peak daily concentrations, and maximum spatial contrasts. Following on our prior study reporting greater spatial contrast in PM$_{2.5}$ and BC concentrations using inversion-focused sampling,[6] we hypothesized that it would also reveal stronger local source contributions in factor analysis, compared with 24-h weeklong sampling.

As in other intra-urban studies,[9,10,17,45] we found substantial spatial variability in constituents, under both the 24-h weeklong and inversion-focused sampling schemes. For constituents that significantly differed by sampling design, concentrations were *consistently higher* using inversion-focused sampling.

As hypothesized, our inversion-focused analyses generally produced clearer and more interpretable factors, and better LUR model fits, compared with the 24-h weeklong method, in both seasons. Most season-specific LUR models were weak (low to
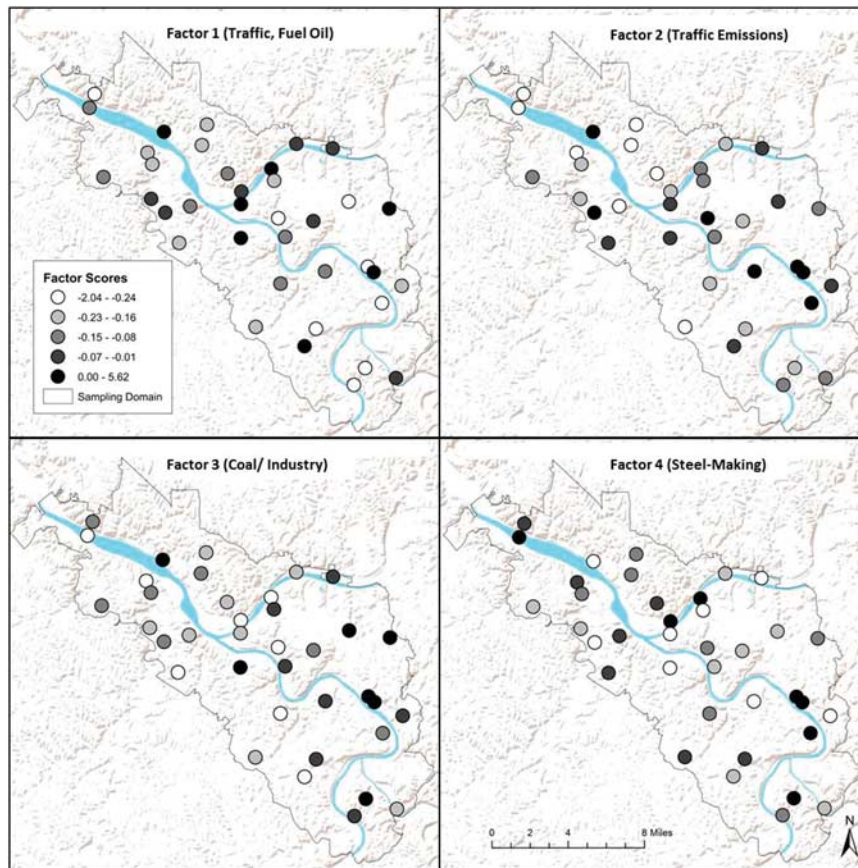
Figure 5. Spatial distribution of factor scores across monitoring locations for *24-h weeklong winter sampling*, based on proposed 4-factor solution.

Table 5. Summer inversion-focused and 24-h weeklong factor score LUR results.

Factor (% prop.)	Proposed sources	Final LUR modeling covariates (R^2)	Covariates most strongly correlated with factor scores (r)
Summer 2011 (Year 1: Inversion-Focused)			
1 (41%)	Soil/Road Dust (Al, Ca, Cr)	VOC emissions (R^2 = 0.26)	VOC emissions (r = 0.33) Elevation within 1000 m (r = − 0.30)
2 (17%)	Brake/Tire (Cd, Cu, Fe, Mn, Ni),	Length of primary and secondary roadways, 1000 m Industrial land use, 1000 m (R^2 = 0.36)	Length of primary and secondary roadways, 1000 m (r = 0.49) Signaled intersections, 1000 m (r = 0.43) Industrial land use, 1000 m (r = 0.34) Elevation within 750 m (r = − 0.51)
3 (9%)	Steel-Making/ Industry (Cs, Mg, Mn, Pb, Zn)	Industrial land use, 750 m (R^2 = 0.34)	Industrial land use, 750 m (r = 0.50) Signaled intersections, 500 m (r = 0.44) Elevation within 750 m (r = − 0.43)
4 (7%)	Coal (As, Se, Tl)	SO$_2$ emissions Signaled intersections, 500 m (R^2 = 0.50)	SO$_2$ emissions (r = 0.53) Signaled intersections, 500 m (r = 0.33)
5 (6%)	Motor Vehicle (P, Zn)	Mean density traffic (primary roads), 1000 m (R^2 = 0.15)	Mean truck density, 1000 m (r = 0.39) Mean density traffic (primary roads), 1000 m (r = 0.38) Length of primary roadway, 1000 m (r = 0.35)
6 (5%)	Diesel/Motor Vehicle (BC, NO$_2$)	Inverse distance to NEI /TRI sites (R^2 = 0.21)	Inverse distance to NEI/TRI sites (r = 0.46) Signaled intersections within 750 m (r = 0.44) Elevation within 1000 m (r = − 0.43)
Summer 2012 (Year 2: 24-h Weeklong)			
1 (38%)	Motor Vehicle (Al, Ba, Ca, P), Brake/Tire (Cu, Sr)	Mean density of bus traffic, 750 m (R^2 = 0.28)	Mean density of bus traffic, 750 m (r = 0.50) Mean density of truck traffic, 750 m (r = 0.50) Mean density traffic (primary roads), 750 m (r = 0.46)
2 (16%)	Steel-Making (Fe, Mn, Zn) Motor Vehicle (BC, Fe, NO$_2$, Zn)	Signaled intersections, 500 m buffer Commercial and industrial land use, 1000 m (R^2 = 0.32)	Signaled intersections, 500 m (r = 0.46) Commercial and industrial land use, 1000 m (r = 0.39) PM$_{2.5}$ emissions (r = 0.25)
3 (10%)	Brake/Tire (Cu, Sr)	Signaled intersections, 500 m (R^2 = 0.47)	Signaled intersections, 500 m (r = 0.36) Population, 1000 m (r = 0.31)
4 (8%)	Coal/Industry (As, Pb, Tl)	SO$_2$ emissions (R^2 = 0.54)	SO$_2$ emissions (r = 0.72)
5 (6%)	Brake/Tire (Cr)	No spatial covariates	SO$_2$ emissions (r = 0.23)
6 (5%)	Coal (Se)	No spatial covariates	No covariates > r = 0.15

Percentage of explained variance is given alongside each factor, along with proposed sources based on literature review, the final LUR covariates (with final R^2), and the covariates that most strongly correlated with the factor scores (rho).

Table 6. Winter inversion-focused and 24-h weeklong factor score LUR results.

Factor (% prop.)	Proposed sources	Final LUR modeling covariates (R^2)	Covariates most strongly correlated with factor scores (r)
Winter 2012 (Year 1: Inversion-Focused)			
1 (44%)	Brake/Tire (Cd, Mg, Sb, Sr, Zn), Soil/Road Dust (Al, Ca, Fe, K, Pb), Steel (Fe, Mn, Pb, Zn)	Commercial and industrial land use, 500 m ($R^2 = 0.18$)	Industrial land use, 1000 m ($r = 0.36$) Elevation within 1000 m ($r = -0.34$) Commercial and industrial land use, 500 m ($r = 0.29$)
2 (12%)	Brake/Tire (Ba, Cr, Cu)	Signaled intersections, 750 m ($R^2 = 0.20$)	Signaled intersections, 750 m ($r = 0.41$) Mean bus density, 500 m ($r = 0.35$)
3 (9%)	Traffic Source (Ce, La, Mo)	Mean density of heavy truck traffic, 500 m Inverse distance to primary roadways ($R^2 = 0.43$)	Mean density of truck traffic, 500 m ($r = 0.36$) Length of primary roadways, 200 m ($r = 0.35$) Traffic density on primary roadways, 300 m ($r = 0.32$)
4 (7%)	Fuel Oil Combustion (Ni)	Distance to nearest primary roadway ($R^2 = 0.23$)	Distance to nearest primary roadway ($r = 0.37$) PM$_{2.5}$ emissions ($r = 0.27$)
5 (5%)	Coal (Se)	Elevation within 50 m ($R^2 = 0.12$)	Elevation within 50 m ($r = -0.33$)
6 (5%)	Diesel/Motor Vehicle (BC)	Signaled intersections, 500 m Industrial land use, 750 m ($R^2 = 0.34$)	Inverse distance to NEI /TRI sites ($r = 0.43$) Signaled intersections, 500 m ($r = 0.42$) Industrial land use, 750 m ($r = 0.38$)
Winter 2013 (Year 2: 24-h Weeklong)			
1 (67%)	Brake/Tire (Cr, Cu, Mg, Sr), Soil/Road Dust (Al, Ca, Cu, Mg), Fuel/Oil (Ni, V)	No spatial covariates	Mean truck density, 500 m ($r = 0.27$) Traffic density of primary roadways, 500 m ($r = 0.26$)
2 (9%)	Diesel/Motor Vehicle (BC, La, NO$_2$, P), Brake/Tire (Ba, Cu, Sb)	Signaled intersections, 500 m PM$_{2.5}$ emissions ($R^2 = 0.30$)	Signaled intersections, 500 m ($r = 0.40$) PM$_{2.5}$ emissions ($r = 0.40$) Mean elevation ($r = -0.40$)
3 (8%)	Coal/Industry (Pb, Se, Tl)	PM$_{2.5}$ emissions ($R^2 = 0.30$)	PM$_{2.5}$ emissions ($r = 0.49$) Commercial and industrial land use, 200 m ($r = 0.38$)
4 (5%)	Steel-Making (Fe, Mn, Zn)	Industrial land use, 500 m ($R^2 = 0.28$)	Industrial land use, 500 m ($r = 0.39$) PM$_{2.5}$ emissions ($r = 0.35$)

Percentage of explained variance is given alongside each factor, along with proposed sources based on literature review, the final LUR covariates (with final R^2), and the covariates that most strongly correlated with the factor scores (rho).

moderate R^2s of 0.15 to 0.54), but reasonably corroborated factor interpretations.

Summer Analyses
Summer sampling revealed greater variability in constituent concentrations, compared with winter, using both sampling designs (Tables 3 and 4), as previously reported for PM$_{2.5}$ and BC.[6] Inversion-focused sampling identified a stronger presence of road-related sources during both seasons, and summer inversion-focused sampling revealed higher concentrations of elements related to steel and coal industries (Table 3). In the summer, we captured a greater contribution from steel and coal emissions under the inversion-focused sampling design than 24-h sampling. LUR models moderately corroborated these factor interpretations, identifying industrial land use for the steel/industry factor ($R^2 = 0.34$) and SO$_2$ emissions for the coal factor ($R^2 = 0.50$) as key spatial covariates. Five of the six summer factors from the 24-h sampling were comprised of elements associated with brake/tire wear or coal burning.

Winter Analyses
Fewer constituents differed by sampling scheme during winter, which was expected, as lower mixing heights and lesser insolation may have reduced the influence of inversion-focused sampling. The clustering of many sources under the first inversion-focused winter factor may be indicative of a low mixing height and combined general traffic and industrial activity, predicted by the summed area of commercial and industrial land use within 500 m. Other factors from the winter inversion-focused analyses were reasonably corroborated using LUR, and by assessing the spatial pattern across sites. Fewer factors were corroborated for the 24-h weeklong sampling design.

Spatial Analyses and Mapping
Spatial modeling and mapping of inversion-focused factor scores generally reinforced factor interpretations, particularly for the inversion-focused samples, as higher loadings of brake and tire wear factors were observed nearer to downtown Pittsburgh, with greater traffic congestion during morning rush hours. Steel-making constituent concentrations were highest in the Braddock neighborhood, near an active steel mill, as in prior studies.[36,39,40] Coal-related constituent concentrations were highest in the neighborhood of Clairton, near the largest coke works in the US; SO$_2$ emissions was a significant predictor for the coal factors under both designs during summer.

The key sources we identified are in keeping with nationwide results using EPA's Chemical Speciation Network (CSN), which, in our region identified factors related to motor vehicle traffic, steel industry, oil combustion, and coal combustion.[33]

Limitations
Owing to equipment availability, both sampling schemes could not be run simultaneously. Although it is possible that the intensity of localized source emissions from traffic and industry

differed in successive years, we established comparability between years, finding similar PM$_{2.5}$ and BC concentrations at the 13 repeated sites. Across both years, reference data at the upwind rural background site were comparable. PM$_{2.5}$ concentrations were similar using each sampling method at the background reference site during both seasons (summer 24-h = 11.92 (SD = 3.99) µg/m^3 *vs* summer inversion-focused = 11.91 (SD = 2.22) µg/m^3); (winter 24-h = 8.43 (SD = 1.76) µg/m^3 *vs* winter inversion-focused = 8.64 (SD = 1.73) µg/m^3). BC results were similar to those found for PM$_{2.5}$ concentrations. We also assessed inversion frequency, and found a comparable number of inversion events by year and season.

A further limitation may be that these elemental constituents comprise only a small fraction of total PM$_{2.5}$ by mass. Sulfur was the most predominant constituent, as in other northeast US studies. For inversion-focused sampling, sulfur accounted for 66% (SD = 14%) of the total characterized elemental mass in summer, and 54% (SD = 12%) in winter. For 24-h weeklong sampling, sulfur accounted for 70% (SD = 10%) and 64% (SD = 11%) of characterized elemental mass in summer and winter, respectively. Sulfur air pollutants (impurity from coal and oil) from power plants include SO$_2$, sulfate PM, and sulfuric acid. SO$_2$ can undergo chemical reactions in the air to form secondary sulfates. Because SO$_2$ emissions from power plants peaked during summer, and warmer temperatures and sunlight generally favor secondary formation, sulfates may be produced more readily, and greater quantities of elemental sulfur taken up into other compounds.

Nonetheless, this 2-year study enabled the comparison of spatial patterning in 24-h weeklong measures *vs* hypothesized high-concentration hours across an urban area. As hypothesized, our inversion-focused sampling approach elucidated greater spatial variability and stronger source contributions. Twenty-four-hour weeklong sampling also produced interpretable factors each season. Inversion-focused sampling captured significantly greater concentrations in several constituents in both seasons, and helped to more clearly distinguish source contributions and reveal peak exposure contrasts across an urban area.[6]

CONFLICT OF INTEREST

The authors declare no conflict of interest.

ACKNOWLEDGEMENTS

REFERENCES

1 Pope CA 3rd, Muhlestein JB, May HT, Renlund DG, Anderson JL, Horne BD. Ischemic heart disease events triggered by short-term exposure to fine particulate air pollution. *Circulation* 2006; **114**: 2443–2448.

2 Mar TF, Jansen K, Shepherd K, Lumley T, Larson TV, Koenig JQ. Exhaled nitric oxide in children with asthma and short-term PM$_{2.5}$ exposure in Seattle. *Environ Health Perspect* 2005; **113**: 1791–1794.

3 Brunekreef B, Dockery DW, Krzyzanowski M. Epidemiologic studies on short-term effects of low levels of major ambient air pollution components. *Environ Health Perspect* 1995; **103**: 3–13.

4 Bell ML. Assessment of the health impacts of particulate matter characteristics. *Res Rep Health Eff Inst* 2012; **161**: 5–38.

5 Bell ML, Dominici F, Ebisu K, Zeger SL, Samet JM. Spatial and temporal variation in PM$_{2.5}$ chemical composition in the United States for health effects studies. *Environ Health Perspect* 2007; **115**: 989–995.

6 Tunno BJ, Michanowicz DR, Shmool JL, Kinnee E, Cambal L, Tripathy S *et al.* Spatial variation in inversion-focused vs 24- h integrated samples of PM and black carbon across Pittsburgh, PA. *J Expo Sci Environ Epidemiol* (e-pub ahead of print 29 April 2015; doi: 10.1038/jes.2015.14).

7 Stanek LW, Sacks JD, Dutto SJ, Dubois JB. Attributing health effects to apportioned components and sources of particulate matter: an evaluation of collective results. *Atmospheric Environment* 2011; **45**: 5655–5663.

8 Clougherty JE, Wright RJ, Baxter LK, Levy JI. Land use regression modeling of intra-urban residential variability in multiple traffic-related air pollutants. *Environ Health* 2008; **7**: 17.

9 Clougherty JE, Houseman EA, Levy JI. Examining intra-urban variation in fine particle mass constituents using GIS and constrained factor analysis. *Atmospheric Environment* 2009; **43**: 5545–5555.

10 de Hoogh K, Wang M, Adam M, Badaloni C, Beelen R, Birk M *et al.* Development of land use regression models for particle composition in twenty study areas in Europe. *Environ Sci Technol* 2013; **47**: 5778.

11 Shmool JL, Michanowicz DR, Cambal L, Tunno B, Howell J, Gillooly S *et al.* Saturation sampling for spatial variation in multiple air pollutants across an inversion-prone metropolitan area of complex terrain. *Environ Health* 2014; **13**: 28.

12 Tunno BJ, Shields KN, Lioy P, Chu N, Kadane JB, Parmanto B *et al.* Understanding intra-neighborhood patterns in PM$_{2.5}$ and PM$_{10}$ using mobile monitoring in Braddock, PA. *Environ Health* 2012; **11**: 76.

13 Wallace J, Corr D, Kanaroglou P. Topographic and spatial impacts of temperature inversions on air quality using mobile air pollution surveys. *Sci Total Environ* 2010; **408**: 5086–5096.

14 Wallace J, Kanaroglou P. The effect of temperature inversions on ground-level nitrogen dioxide (NO$_2$) and fine particulate matter (PM$_{2.5}$) using temperature profiles from the Atmospheric Infrared Sounder (AIRS). *Sci Total Environ* 2009; **407**: 5085–5095.

15 ISO TC 146/SC3. ISO 9835:1993, Ambient air - Determination of a black smoke index. In 1993.

16 Sutton KL, Caruso JA. Liquid chromatography-inductively coupled plasma mass spectrometry. *J Chromatogy A* 1999; **856**: 243–258.

17 Levy JI, Clougherty JE, Baxter LK, Houseman EA, Paciorek CJ. HEI Health Review Committee Evaluating heterogeneity in indoor and outdoor air pollution using land-use regression and constrained factor analysis. *Res Rep Health Eff Inst* 2010; **152**: 5–80.

18 Brown S, Eberly S, Paatero P, Norris G. Methods for estimating uncertainty in PMF solutions: examples with ambient air and water quality data and guidance on reporting PMF results. *Sci Total Environ* 2015; **518**: 626–635.

19 Apeagyei E, Bank MS, Spengler JD. Distribution of heavy metals in road dust along an urban-rural gradient in Massachusetts. *Atmospheric Environment* 2011; **45**: 2310–2323.

20 Figi R, Nagel O, Tuchschmid M, Lienemann P, Gfeller U, Bukowiecki N. Quantitative analysis of heavy metals in automotive brake linings: a comparison between wet-chemistry based analysis and in-situ screening with a handheld X-ray fluorescence spectrometer. *Anal Chim Acta* 2010; **676**: 46–52.

21 Brunekreef B, Janssen NA, de Hartog J, Harssema H, Knape M, van Vliet P. Air pollution from truck traffic and lung function in children living near motorways. *Epidemiology* 1997, 298–303.

22 Iijima A, Sato K, Yano K, Kato M, Kozawa K, Furuta N. Emission factor for antimony in brake abrasion dusts as one of the major atmospheric antimony sources. *Environ Sci Technol* 2008; **42**: 2937–2942.

23 Gietl JK, Lawrence R, Thorpe AJ, Harrison RM. Identification of brake wear particles and derivation of a quantitative tracer for brake dust at a major road. *Atmospheric Environment* 2010; **44**: 141–146.

24 Sternbeck J, Sjödin Å, Andréasson K. Metal emissions from road traffic and the influence of resuspension—results from two tunnel studies. *Atmospheric Environment* 2002; **36**: 4735–4744.

25 Schauer JJ. Evaluation of elemental carbon as a marker for diesel particulate matter. *J Expo Sci Environ Epidemiol* 2003; **13**: 443–453.

26 Irvine KN, Perrelli MF, Ngoen-klan R, Droppo IG. Metal levels in street sediment from an industrial city: spatial trends, chemical fractionation, and management implications. *Journal of Soils and Sediments* 2009; **9**: 328–341.

27 Lee S, Liu W, Wang Y, Russell AG, Edgerton ES. Source apportionment of PM$_{2.5}$: comparing PMF and CMB results for four ambient monitoring sites in the southeastern United States. *Atmospheric Environment* 2008; **42**: 4126–4137.

28 Li Z, Hopke PK, Husain L, Qureshi S, Dutkiewicz VA, Schwab JJ *et al.* Sources of fine particle composition in New York city. *Atmospheric Environment* 2004; **38**: 6521–6529.

29 Lough GC, Schauer JJ, Park J-S, Shafer MM, DeMinter JT, Weinstein JP. Emissions of metals associated with motor vehicle roadways. *Environ Sci Technol* 2005; **39**: 826–836.

30 Ogulei D, Hopke PK, Zhou L, Patrick Pancras J, Nair N, Ondov JM. Source apportionment of Baltimore aerosol from combined size distribution and chemical composition data. *Atmospheric Environment* 2006; **40**: 396–410.

31 Qin Y, Kim E, Hopke PK. The concentrations and sources of PM$_{2.5}$ in metropolitan New York City. *Atmospheric Environment* 2006; **40**: 312–332.

32 Rizzo MJ, Scheff PA. Fine particulate source apportionment using data from the USEPA speciation trends network in Chicago, Illinois: comparison of two source apportionment models. *Atmospheric Environment* 2007; **41**: 6276–6288.

33 Thurston GD, Ito K, Lall R. A source apportionment of US fine particulate matter air pollution. *Atmospheric Environment* 2011; **45**: 3924–3936.

34 Zhao W, Hopke PK, Norris G, Williams R, Paatero P. Source apportionment and analysis on ambient and personal exposure samples with a combined receptor model and an adaptive blank estimation strategy. *Atmospheric Environment* 2006; **40**: 3788–3801.

35 Hammond DM, Dvonch JT, Keeler GJ, Parker EA, Kamal AS, Barres JA *et al*. Sources of ambient fine particulate matter at two community sites in Detroit, Michigan. *Atmospheric Environment* 2008; **42**: 720–732.

36 Pekney NJ, Davidson CI, Bein KJ, Wexler AS, Johnston MV. Identification of sources of atmospheric PM at the Pittsburgh Supersite, Part I: single particle analysis and filter-based positive matrix factorization. *Atmospheric Environment* 2006; **40**: 411–423.

37 Lough GC, Schauer JJ. Sensitivity of source apportionment of urban particulate matter to uncertainty in motor vehicle emissions profiles. *J Air Waste Manag Assoc* 2007; **57**: 1200–1213.

38 Spencer MT, Shields LG, Sodeman DA, Toner SM, Prather KA. Comparison of oil and fuel particle chemical signatures with particle emissions from heavy and light duty vehicles. *Atmospheric Environment* 2006; **40**: 5224–5235.

39 Aneja VP, Isherwood A, Morgan P. Characterization of particulate matter (PM$_{10}$) related to surface coal mining operations in Appalachia. *Atmospheric Environment* 2012; **54**: 496–501.

40 Heal MR, Hibbs LR, Agius RM, Beverland IJ. Interpretation of variations in fine, coarse and black smoke particulate matter concentrations in a northern European city. *Atmospheric Environment* 2005; **39**: 3711–3718.

41 Salvador P, Artinano B, Querol X, Alastuey A. A combined analysis of backward trajectories and aerosol chemistry to characterise long-range transport episodes of particulate matter: the Madrid air basin, a case study. *Sci Total Environ* 2008; **390**: 495–506.

42 Gunawardana C, Goonetilleke A, Egodawatta P, Dawes L, Kokot S. Source characterisation of road dust based on chemical and mineralogical composition. *Chemosphere* 2012; **87**: 163–170.

43 Lall R, Thurston GD. Identifying and quantifying transported vs. local sources of New York City PM$_{2.5}$ fine particulate matter air pollution. *Atmospheric Environment* 2006; **40**: 333–346.

44 Viana M, Kuhlbusch T, Querol X, Alastuey A, Harrison R, Hopke P *et al*. Source apportionment of particulate matter in Europe: a review of methods and results. *Journal of Aerosol Science* 2008; **39**: 827–849.

45 Clougherty JE, Kheirbek I, Eisl HM, Ross Z, Pezeshki G, Gorczynski JE *et al*. Intra-urban spatial variability in wintertime street-level concentrations of multiple combustion-related air pollutants: the New York City Community Air Survey (NYCCAS). *J Expo Sci Environ Epidemiol* 2013; **23**: 232–240.

46 Aneja VP, Isherwood A, Morgan P. Characterization of particulate matter (PM$_{10}$) related to surface coal mining operations in appalachia. *Atmos Environ* 2012; **54**: 496–501.

47 De Foy B, Smyth AM, Thompson SL, Gross DS, Olson MR. Sources of nickel, vanadium and black carbon in aerosols in Milwaukee. *Atmos Environ* 2012; **59**: 294–301.

48 Schauer JJ, Lough GC, Schafer MM, Christensen WF, Arndt MF, DeMinter JT *et al*. Characterization of metals emitted from motor vehicles, HEI Research Reports, Boston, 2006.

49 Fine PM, Cass GR, Simoneit BRT. Chemical characterization of fine particle emissions from fireplace combustion of woods grown in the northeastern United States. *Environ Sci Tech* 2001; **35**: 2665–2675.

50 Salvador P, Artinano B, Querol X, Alastuey A. A combined analysis of backward trajectories and aerosol chemistry to characterise long-range transport episodes of particulate matter: the Madrid air basin, a case study. *Sci Total Environ* 2008; **390**: 495–506.

Supplementary Information accompanies the paper on the Journal of Exposure Science and Environmental Epidemiology website (http://www.nature.com/jes)